Tethered Fixed-Wing Aircraft to Lift Payloads: A Concept Enabled by Electric Propulsion

David Rancourt

Université de Sherbrooke
3000 boul. Université – Pavillon P2
Sherbrooke, QC
CANADA

david.rancourt2@usherbrooke.ca

Etienne Demers Bouchard

Georgia Institute of Technology
275 Ferst Drive NW
Atlanta, GA
USA

etienne.demersb@gatech.edu

Keywords: Electric propulsion, novel aircraft concept, VTOL, hybrid-electric powertrain

ABSTRACT

Helicopters have been essential to the military as they have been one of the only solutions for air-transporting substantial payloads with no need for complex mile-long runway infrastructures. However, they are fundamentally limited with high fuel consumption and reduced range. A disruptive concept to vertical lift uses tethered fixed-wing aircraft to lift a payload, where multiple aircraft collaborate and fly along a near circular flight path in hover. The Electric-Powered Reconfigurable Rotor concept (EPR^2) leverages the recent progress in electric propulsion and modern controls to enable efficient load lifting using fixed-wing aircraft. The novel idea is to replace tethered manned aircraft (with onboard energy, fuel) with electric-powered fixed-wing aircraft with remote energy source to enable efficient collaborative load lifting. This paper presents the conceptual design of a heavy-lifting aircraft concept using electric-powered tethered fixed-wing aircraft for a ~30 metric ton lifting capability. A physics-based multidisciplinary design and simulation environment is used to predict the performance and optimize the aircraft flight path. It is demonstrated that this concept could hover with only 3.01 MW of power yet be able to translate to over 80 kts with minimal power increase by leveraging the benefits of complex non-circular flight paths. Powered with a series-hybrid powertrain, this design could hover in excess of 12 hours with a fuel capacity of 6 000 kg. Future work includes experimental flight tests of subscale models including control optimization.

1.0 INTRODUCTION

Helicopters have been essential to the military as they have been one of the only solutions for air-transporting substantial payloads with no need for complex mile-long runway infrastructures. Recent developments for helicopters have focused on increasing cruising speed and cruise efficiency with novel concepts such as the Sikorsky X-2 and the V-22 Osprey rather than increasing hovering efficiency. Still, there is a need for a highly efficient hovering aircraft to support heavy cargo delivery (Ardema, 1981) and ship unloading, improve telecommunications using “pseudo-satellite” networks, and provide various aerial support (Brown, 1981; Heatley, 1985; Rajendran, Masral and Kutty, 2017). Airships and hybrid airships have been proposed to provide a high lifting capacity with minimal runway requirement (Carichner and Nicolai, 2013). However, they are fundamentally limited with wind sensitivity, storage complexity, limited maneuverability, and complex weight management during unloading.

A disruptive concept to vertical lift uses tethered fixed-wing aircraft to lift a payload, where multiple aircraft collaborate and fly along a near circular flight path in hover. Such approach has the potential to reduce the power requirement in hover due to the much larger disk area covered by the “blades”, and improve cruise efficiency compared to rotary-wing aircraft. However, most conceptual designs and flight tests to demonstrate this concept used manned aircraft powered by conventional fuel with kilometer-long tethers (Williams and

Trivailo, 2007b, 2007a; Wilson and Bennet, 1983; Wilson Jr., 1983). The airplane flight paths were limited to simple circles at near constant airspeed with minimal capacity to hover in the presence of wind (Williams, 2010). Wilson from Lockheed evaluated that the lifting capability of two C130 aircraft would only reach 9 000 kg, equivalent to 25% the empty weight of a single aircraft due to the complex deorbiting process from hover to forward flight, since any translation would require the multiple aircraft to fly in the same direction (Wilson and Bennet, 1983). Under those limitations and coordination complexity between aircraft, this concept has never been used.

The Electric-Powered Reconfigurable Rotor concept (EPR^2) leverages the recent progress in electric propulsion and modern controls to enable efficient load lifting using fixed-wing aircraft. The novel idea is to replace tethered manned aircraft (with onboard energy, fuel) with electric-powered fixed-wing aircraft with remote energy source to enable efficient collaborative load lifting. By keeping the energy source (battery and/or generator) in the "fuselage" section, the lightweight airplanes have an increased agility and thrust-to-weight ratio allowing for a true vertical takeoff as illustrated in Figure 1-1a. A three-airplane configuration is preferred to enhance payload control, and additional aircraft could increase reliability in case of an airplane failure.

Figure 1-1 illustrates the three phases of flight of this concept. After a vertical takeoff in a tailsitting configuration or a "quadplane" approach, the aircraft transition to a periodic (not necessary circular) flight path and lift the fuselage as depicted in Figure 1-1b. The use of electric motors on agile aircraft is an enabler for the tethered aircraft to perform complex flight path, defined as non-circular with continuous variation in airspeed, aircraft attitude, and tether tension. Figure 1-1c illustrates an example of an optimized complex flight path of the three airplanes and the payload for a 15 m/s translational speed (Rancourt, Demers Bouchard and Mavris, 2016).

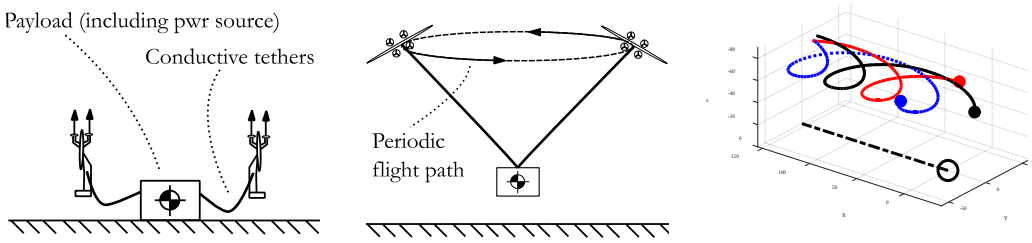

a) Takeoff phase b) Vertical flight c) forward flight

Figure 1-1: Representation of the flight phases and an example of a complex flight path during motion

One of the main advantages of this concept over conventional rotorcraft consists of its reduced power requirement in hover or near hover. Demers Bouchard demonstrated using a multidisciplinary environment that two 20 kW electric aircraft with a wingspan of 8 m could lift a fuselage of 800 kg in hover (Demers Bouchard, Rancourt and Mavris, 2015). This initial study focused on the optimization of aircraft flight path and tether length, while the tethered airplanes were assumed to be very similar to the Makani Wing 7 airplanes developed for the airborne wind energy sector (Makani Power, 2011), shown in Figure 1-2. A latter study by the same authors evaluated the benefits to perform complex flight paths compared to circular flight paths during translation of the system (Rancourt, Demers Bouchard and Mavris, 2016). Using the same test case, it was shown that tethered airplane complex flight paths could reduce electrical power requirement by as much as 40% compared to circular flight paths. Since each aircraft is independent, their flight speed can be adapted as a function of the "rotor" azimuthal position and the lift requirement can be transferred between each aircraft, resulting in a higher rotor efficiency. This work also highlighted the need for electric powered aircraft with

turboelectric generators in the payload bay since complex flight paths require periodic variations in the power requirement reaching 50% every few seconds for each individual aircraft.

Figure 1-2: Makani Wing 7 aircraft during takeoff

In addition to reduced power requirements, the EPR[2] concept has the potential to show (1) reduced maintenance cost due to the reduced cyclic loads on the "rotor" similar to the airborne wind energy sector, (2) minimal vibration of the payload thanks to the tether damping, (3) avoid brownout or whiteout during hover due to minimal induced velocity, (4) vertical autorotation capability and no risk for the vortex-ring state. These characteristics could be highly beneficial in military applications.

This paper presents the conceptual design of a heavy-lifting aircraft concept using electric-powered tethered fixed-wing aircraft for a ~30 metric ton lifting capability. Aircraft performance across the entire flight envelope is demonstrated, from hover to complex non-circular flight path across different air density and payload mass. In particular, this paper demonstrates the benefits of electric propulsion and highly flexible aircraft flight paths in reducing power requirement and expanding military capability compared to alternative concepts.

2.0 METHODOLOGY

Due to the significant difference in the aerodynamics and dynamics of vertical and forward flight, two different multidisciplinary design and optimization environments are used to predict the system performance. An inverse dynamics approach minimizes the required feedback in the modeling and simulation environment while providing the desired performance metrics. Both MDO environments attempt to minimize the power requirement in flight by optimizing the tethered airplane flight paths. The vertical flight MDO is presented second since it represents a simplified case of the forward flight with an adapted aerodynamic model.

2.1 Forward Flight

Figure 2.1-1 presents the general design structure matrix (DSM) used to solve for the minimum power requirement given a target fuselage trajectory. The remainder of this section details each model and their assumptions and how the interdisciplinary coupling is solved.

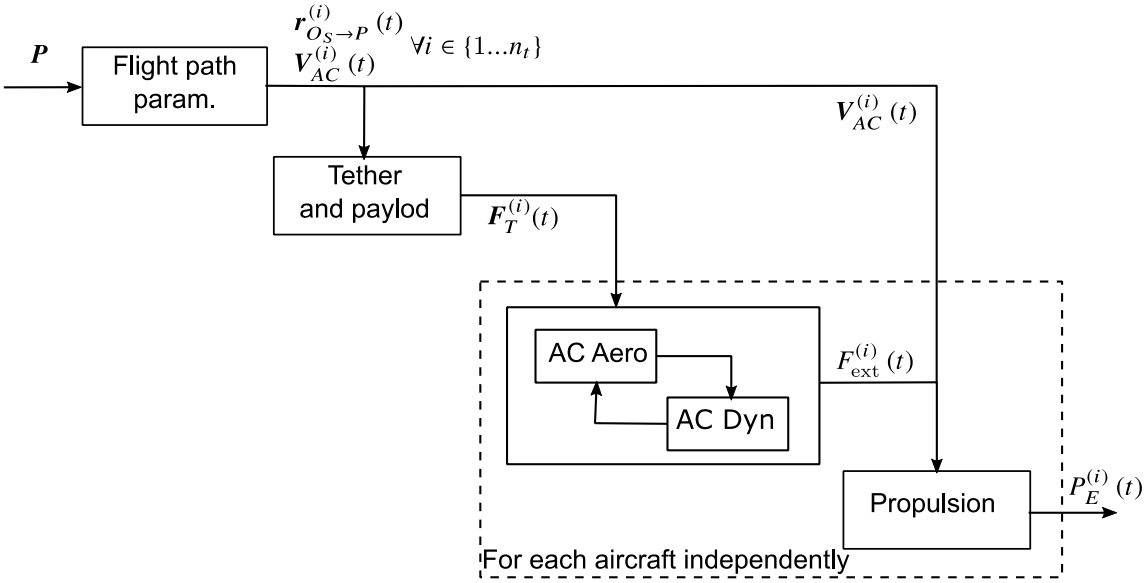

Figure 2.1-1: DSM for forward flight

2.1.1 Flight Path Parameters

Let S be the system-carried frame (North-East-Down) defined at the fuselage position and $B^{(i)}$ be the i-th aircraft body frame defined in the conventional approach. The objective of the parameterization model is to represent the three tethered airplane position vectors $\mathbf{r}_{O_S \to P_i}$ in the system-carried frame into a representation with fewer parameters as shown in Eqn (1)

$$\mathbf{P} = f\left(\mathbf{r}_{O_S \to P_i}^{(i)}(t)\right) \forall i \in \{1,2,3\} \tag{1}$$

where **P** is a small set of parameters without time dependence. In this study, the position vector of the three aircraft is completely represented using only 7 variables. Complete details about this transformation can be found in (Rancourt, 2016) but a summary is provided herein for completeness.

First, the airplane flight path is defined on a plane using the major and minor axes of an ellipse, normalized by the tether length,

$$\frac{x^2}{a_1^2} + \frac{y^2}{a_2^2} = L_{tether}^2 \tag{2}$$

where a_1 and a_2 are the two ellipse parameters. For a fixed fuselage position over time, the flight path has to be adjusted to maintain a constant distance with the fuselage. This transformation is done by projecting the flight path on a sphere of radius L_{tether} centered on the fuselage, as presented in Figure 2.1-2.

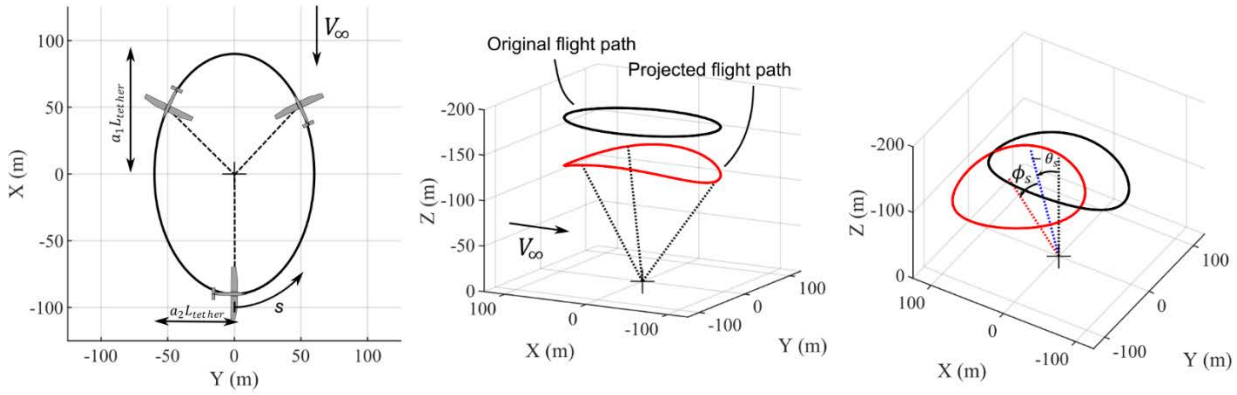

Figure 2.1-2: Summary of the flight path trajectory transformations

Second, the tethered airplane flight speed with respect to the fuselage along the trajectory is defined using three parameters: the mean flight speed V_m and two parameters defining a variation about the mean flight speed along the flight path, V_{1c} and V_{1s}. Let s be the normalized flight path distance from the reference $0 \leq s \leq 1$. The variation in aircraft flight speed with respect to s is

$$V_{AC}(s) = \frac{V_m}{k}(1 + V_{1c}\cos(2\pi s) + V_{1s}\sin(2\pi s)) \tag{3}$$

where k is a parameter that enforce the mean aircraft flight speed to be V_m. A positive of V_{1c} defines a faster airplane on the advancing side, and a positive value of V_{1s} defines a faster airplane on front section of the "rotor".

Finally, the whole flight path can be tilted similar to conventional rotor flapping angles. A first rotation θ_s about the Y-axis tilt backward the flight path, followed by a lateral inclination ϕ_s where a positive value tilts the reference axis of rotation to the left. An airplane flight path closer to the fuselage on the advancing side alleviates the consequences of the varying relative wind speed as shown in the results section. The three airplanes are separated by a one third of a period defined in time.

In summary, the three periodic airplane flight paths in the vehicle carried frame are completely defined using seven variables, namely $a_1, b_1, V_m, V_{1c}, V_{1s}, \phi_s, \theta_s$. The local relative velocity with respect to the air is denoted $\boldsymbol{V}_{AC}^{(i)}(t)$ and include the contribution of the freestream velocity in forward flight V_∞.

2.1.2 Tether and Fuselage Dynamic Model

The coupled tether and fuselage dynamics model is loosely inspired from the work of Williams, based on a lumped-mass model adapted for a rigid tether model (Williams and Ockels, 2009). Given the prescribed periodic aircraft kinematics $\mathbf{r}_{O_S \to P_i}^{(i)}(t)$ and the local relative wind velocity $\boldsymbol{V}_{AC}^{(i)}(t)$ (including the contribution of the external wind V_∞), the force applied on each airplane $\boldsymbol{F}_T^{(i)}(t)$ is evaluated. This last result is used as an input to the aircraft dynamic and aerodynamic model.

For performance prediction only, a previous work by the author (Rancourt, 2016) demonstrated that a rigid tether model shows an error of only 0.8% in the dissipated aerodynamic power by tether in vertical flight compared to a fully elastic lumped mass model while reducing the computational time by 2 orders of magnitude. To remain true, the flight paths would have to be slightly modified to maintain an applied force on

each airplane $\boldsymbol{F}_T^{(i)}(t)$ after consideration for the tether elasticity. This "compensation" for tether elasticity and curvature is outside the scope of this paper.

The tether aerodynamic drag is evaluated using the model proposed by Hoerner based on the crossflow principle (Hoerner, 1992). The lift and drag coefficients for an inclined cylinder are given by Eqns (4-5)

$$C_{D,tether} = C_f + C_n|\sin^3\gamma| \tag{4}$$

$$C_{L,tether} = C_n \sin^2\gamma\cos\gamma \tag{5}$$

where γ is the angle between the tether section and the relative wind velocity. The skin-friction drag and the crossflow coefficient are obtained using Eqns (6-7)

$$C_f = 0.038 - 0.0425M_p \tag{6}$$

$$C_n = 1.17 + \frac{M_n}{40} - \frac{M_n}{4} + \frac{5M_n}{8} \tag{7}$$

where M_n is the normal Mach number, and M_p the tangential Mach number on the tether. For the vertical flight phase the relative wind velocity at the payload is near zero, and the tethered airplanes follow a circular flight path. In this case, the tether lift is reduced to zero ($C_{L,tether} = 0$) since the flow is always normal to the tether segment. The tether aerodynamics is evaluated for each discretized tether segments, in order to capture the variation in aerodynamics as a function of the tether location.

The fuselage is modeled as a point mass, and its aerodynamics is reduced to a force aligned with the local freestream velocity, evaluated using an equivalent flat plate area approach. Inertial reactions of the tethers are obtained by applying Newton's law on each rigid tether segment and by adding the gravitational forces.

Under the assumption of rigid tethers, the proposed flight path parameterization enforces no fuselage motion in the vehicle carried frame, which reduces the computational time. Moreover, three airplanes provide a deterministic payload position, simplifying the calculation.

2.1.3 Coupled Airplane Dynamics and Aerodynamics Model

The objective of the coupled aerodynamic and dynamic aircraft model is to evaluate the required aerodynamic forces (lift and thrust) and the thrust required $F_{ext}^{(i)}(t)$ given the prescribed flight path $\mathbf{r}_{O_S\to P_i}^{(i)}(t)$ and the tether forces $\boldsymbol{F}_T^{(i)}(t)$ as a function of time. A simple point-mass model is assumed for the aircraft and the approximation of the lifting line aerodynamic model is assumed to evaluate the drag as shown in Eqn (8)

$$\boldsymbol{D}_{AC}^{(i)} = \frac{1}{2}\rho\left(\frac{C_L^2}{\pi Ae} + C_{D_0}\right)|\boldsymbol{V}_{AC}|\,\boldsymbol{V}_{AC}\,S \tag{8}$$

where S denotes the wing area, e denotes the Oswald efficiency factor, and C_{D_0} denotes the airplane parasitic drag. The result is a set of five coupled equations with five unknowns: thrust, drag, lift, bank angle, and lift coefficient. The approach presented above is valid if the wake interaction between the airplanes is neglected, limiting its usage in forward flight as shown in Figure 1-1c. An alternate model is proposed for vertical flight further in this article.

2.1.4 Propulsion Model

A conservative powertrain efficiency of 90% is assumed (Toliyat and Kliman, 2004) and the propeller efficiencies are set to 80% while creating thrust, and reduced to 70% during power harvesting. This later flight condition occurs for flight conditions where the airplane has to dissipate energy such as a rapid deceleration during non-circular flight paths. Finally, the resistive losses in the tether are evaluated using Ohms's law using the conductor properties at room temperature.

2.2 Vertical Flight

Figure 2.2-1 presents the general design structure matrix (DSM) used to solve for the power requirement given a target payload in vertical flight. This flight phase is characterized by circular flight path of the tethered airplane at a constant flight speed $V_{AC} = |\boldsymbol{V}_{AC}|$, where the power requirement is constant in time and equal for each airplane. The flight path radius is defined using the variable $a = a_1 = a_2$ as defined for the forward flight. The payload remains still and there is no horizontal wind affecting the system. The tether aerodynamics and dynamics model and the propulsion model remain unchanged if compared to the forward flight. However, an approximation of the lifting line method for the aerodynamics model cannot be used in hover since it underpredicts the airplane drag by neglecting the lifting surface wake interaction represented by the vertical induced velocity. The remainder of this section details the differences in the aerodynamics model to capture the self-induced velocity.

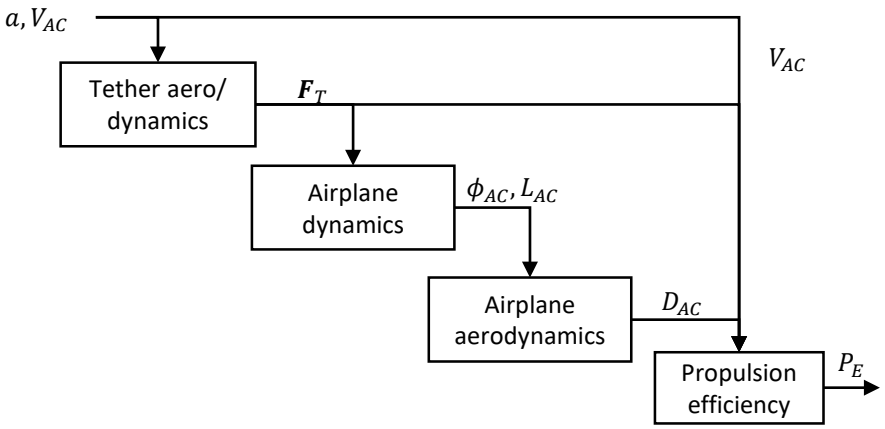

Figure 2.2-1: Design structure matrix for the vertical flight case

2.2.1 Aerodynamics of the Vertical Flight

The objective of the wing aerodynamics model in vertical flight is to evaluate the airplane drag D_{AC}, airplane pitch θ_0, and aileron deflection δ_a to maintain a circular flight path of radius $a \cdot L_{tether}$ at flight speed V_{AC} with a target lift L_{AC}.

In hover or during vertical flight, strong similarities exist between a conventional helicopter rotor and the EPR[2] "rotor" system comprised of three (or more) fixed-wing aircraft. First, the airplanes remain at equal angular distance in hover. Second, both the wings and blades have a high aspect ratio with low solidity. Third, the wings and blades operate in the wake of the other lifting surfaces. Figure 2.2-2 illustrates the concept.

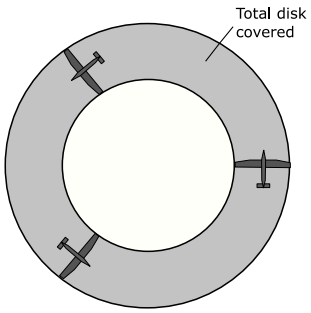

Figure 2.2-2: Equivalent disk area covered by the circling airplanes in hover

The "rotor" aerodynamics is therefore modeled using a blade-element-momentum theory (BEMT) (Johnson, 2013), where each airplane represent the outer part of a conventional rotor blade. The BEMT balances accuracy and computational time in a design space exploration context. Previous studies by the author validated this approach using free vortex wake methods and observed similar variations in the power requirement across the design space (Rancourt, 2016). Tip and root losses are considered using Prandlt root and tip loss models and includes a conservative parasitic drag coefficient for the blade "airfoils". The angular induction is neglected due to the reduce rotor solidity. The effect of the airplane bank angle (below 20 deg) is neglected on the BEMT formulation. Aileron effects are evaluated by changing the airfoil properties in the selected region, creating a rolling moment about the airplane center of mass.

3.0 BASELINE AIRCRAFT

Over the last decade, significant research and development efforts have been invested to bring to the market an efficient airborne wind energy concept. Makani (now an independent company under Alphabet) designed and recently demonstrated a continuous power generation of 600 kW with their M600 wing, presented in Figure 3-1.

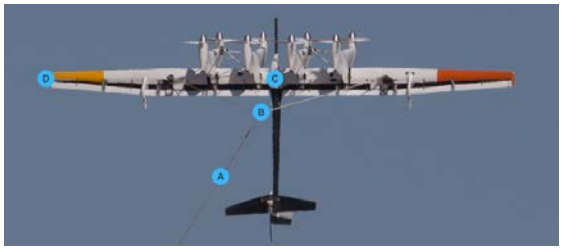

Figure 3-1: M600 aircraft by Makani (*https://makanipower.com/technology/*)

The Makani M600 is used as a baseline aircraft due to strong similarities between the operating condition of this aircraft and the EPR2 concept, especially in a heavy lifting concept. The baseline aircraft and tether characteristics were obtained from the public domain (Makani Power, 2011).

In this work, an increase of near 50% in the airplane mass is applied as a conservative measure to increase the structural mass and increase in electrical powertrain power to 1.5 MW. The wingspan is reduced to 20 m to reduce the ground footprint while increasing the structural stiffness of the structure. Conservative values are

used as a mitigation action since a preliminary design of the wing under those conditions is not available. However, a sensitivity to the wing mass is provided in the results section to quantify the effect of the mass assumption. Table 3-1 first outlines the airplane characteristics.

Table 3-1: Fixed-wing airplane characteristics

Characteristics	Value
Airplane mass	1500 kg
Wingspan	20 m
Aspect ratio	10
Oswald efficiency factor	0.85
Zero lift drag coefficient	0.02
Maximum lift coefficient	1.8

The tether characteristics exposed in Table 3-2 are also conservative compared to the baseline system. First, the linear mass is increased from 0.55 kg/m (Makani Power, 2011) to 1 kg/m to consider the increase in tether loads. A fixed tether length of 150 m is used which equals to 7.5 times the airplane wingspan, a value similar to an EPR2 subscale flight test experimental setup (Chapdelaine, Ledoux and Rancourt, 2019). An 8000 V DC power transmission is used as for the M600 aircraft.

Table 3-2: Tether characteristics.

Characteristics	Value
Conductor diameter	6.35 mm
DC Voltage	8000 V
External diameter	20 mm
Linear mass	1 kg/m
Length	150 m

4.0 OPTIMIZATION PROBLEM

For each flight speed, the aircraft flight path (fully defined by a fixed set of parameters $\boldsymbol{P}$) is optimized to minimize the mean electrical power requirement of the three aircraft, as formulated hereafter, where t_i and t_f defines the initial and final time for 1 complete rotor period.

Minimize $\quad P_{mean}(\boldsymbol{P}) = \frac{1}{t_f - t_i}\int_{t_i}^{t_f} P_E(\boldsymbol{P}, t)dt$

Subject to - Constraints in the flight path parameters (side constraints)

- $\max[C_L(t)]_{t_i}^{t_f} \leq C_{L,max}$

Given - Aircraft geometry and properties

- Fuselage mass

- Tether length

- System flight speed and atmospheric conditions

For the vertical flight case defined with a circular flight path at constant speed, only two flight path parameters are considered: a, the normalized flight path radius and V_m, the mean flight speed. For the forward flight case, seven variables fully define the flight path as described in the methodology section ($a_1, b_1, V_m, V_{1c}, V_{1s}, \phi_s, \theta_s$).

5.0 RESULTS

5.1 Baseline System Performance

Figure 5.1-1 presents the optimized power curve including the takeoff, hover, and forward flight with a 30-ton fuselage at standard atmospheric conditions.

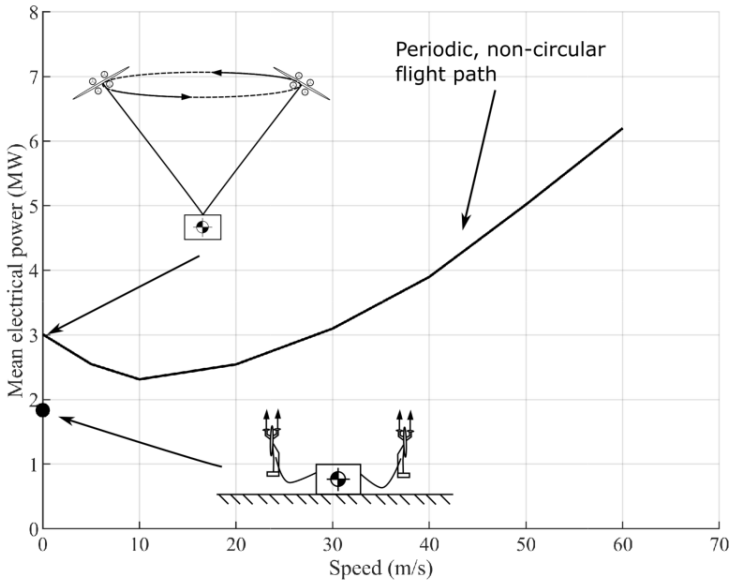

Figure 5.1-1: EPR2 electrical power curve for a 30-ton fuselage.

Under those conditions, 3.01 MWe is required from the fuselage to vertically lift a 30-ton fuselage, which include the hybrid powertrain, the energy source (battery and fuel), and the actual payload.

The minimal hover power requirement is achieved with a constant airplane flight speed of 58.1 m/s and a normalized flight path radius $a_1 = 0.598$. The roll equilibrium is maintained by a constant aileron deflection of 15 degrees, which are located on the outer 18% span. Compared to conventional rotorcraft, the equivalent induced velocity in the rotor plane averages 4 m/s due to the equivalent 11 000 m^2 disk area, approximately 20 times higher than the Sikorsky CH-53E heavy lift helicopter. Including the tip losses, the total induced power reaches 1.6 MW. Figure 5.1-2 illustrates the system power breakdown in hover.

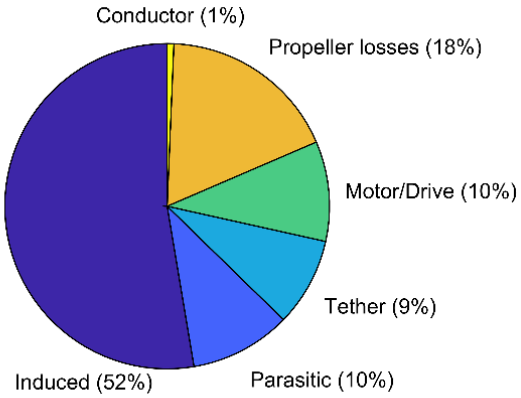

Figure 5.1-2: Loss mechanisms in hover

As expected from the powertrain efficiency, approximately 10% of the losses are attributed to the electric motor and drive, while the Joule losses in the conductors are reduced to only 10 kW due to the high voltage. The wing parasitic losses reaches 10% (304 kW) attributed to the wing's C_{D0}. Finally, the tether drag only accounts for 9 % of the power losses.

The forward flight path illustrates the salient benefits of the EPR^2 technology, with highly flexible flight path to avoid the effect of the reverse flow. Figure 5.1-3 illustrates the optimized flight path for a 20 m/s wind speed.

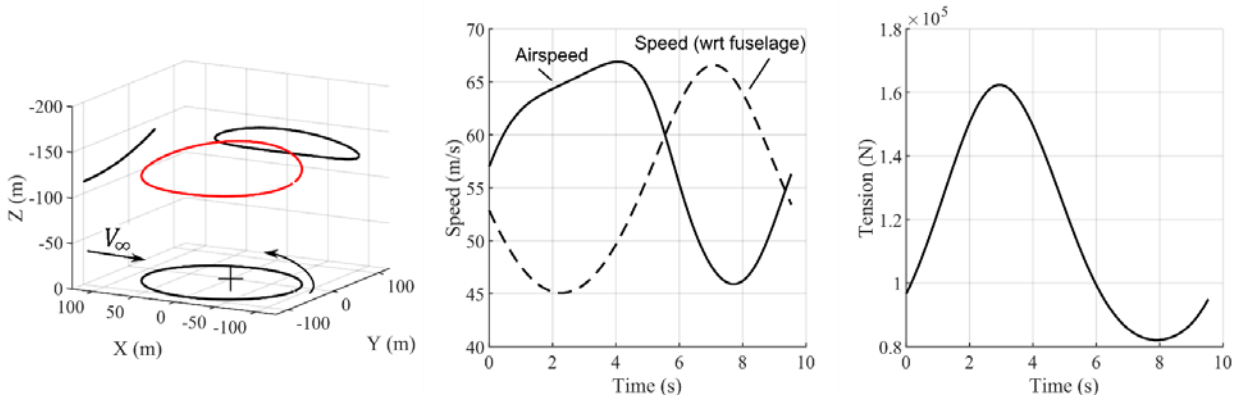

Figure 5.1-3: Optimised flight path and salient flight parameters at 20 m/s

As the airplane travels against the wind in the first few seconds of the flight path, the airspeed is 11 m/s higher than the mean flight speed with a flight trajectory closer to the fuselage from a top view. In a 3-airplane configuration, this position increases the tension in the tether to maintain the fuselage in an equilibrium state, as shown in Figure 5.1-3. This approach minimizes the aerodynamic losses by maintaining the airplane near its optimal lift-to-drag ratio even if the airspeed is higher than average. The optimal airplane flight speed with respect to the fuselage is 18% lower on the advancing side of the flight path, yet the airspeed remains higher than average. The opposite situation can be observed on the retreating side, where the airplane airspeed is reduced therefore limiting the lifting capability. However, this lower position compared to the advancing side reduces the lift requirement on the airplane – an ideal situation to maintain a near constant lift coefficient.

The optimized flight path created strong variations in the power requirement for each airplane as a function of time. Figure 5.1-4 presents the individual power requirement by airplane and the total power requirement along the optimal flight path which minimizes the mean power requirement by the system.

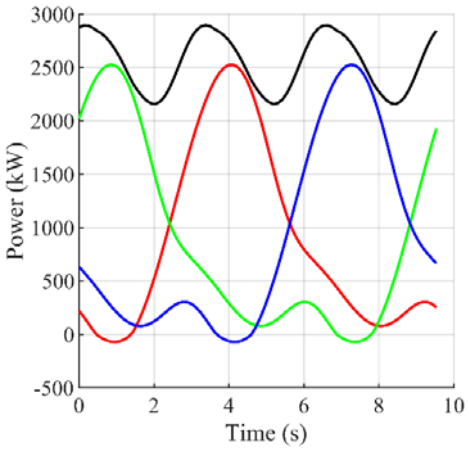

Figure 5.1-4: Electrical power requirement variation as a function of time for each airplane (the red curve is associated with the airplane with the initial position at $y = 0$ and $x = -100$ at $t = 0$).

As the airplane transitions from the retreating side to the advancing side, the flight speed with respect to the inertial frame reduces, causing a reduction in the power requirement to near zero. However, the transition from the advancing side to the retreating side requires a peak power requirement near 2.5 MW to accelerate the airplane from 45 m/s to 65 m/s within 4 seconds. Similar observations can be done throughout the flight envelope with positive flight speed. Electric and series-hybrid electric propulsion technologies are ideal to support the periodic variation in power requirement

Finally, the takeoff phase requires 1.9 MW of electrical power to vertically lift the three tethered airplanes using the thrust generated by their 8, 1-meter diameter propeller, a value lower than the hover and forward flight phase.

5.2 Sensitivity to Air Density and Rotor Reconfiguration

One of the salient advantages of the EPR^2 concept is the ability to reconfigure the “rotor” based on the flight condition to minimize the power requirement. Figure 5.1-5 illustrates the effect of reduced density operations on the lifting capability of circling tethered airplanes and the associated optimal flight path.

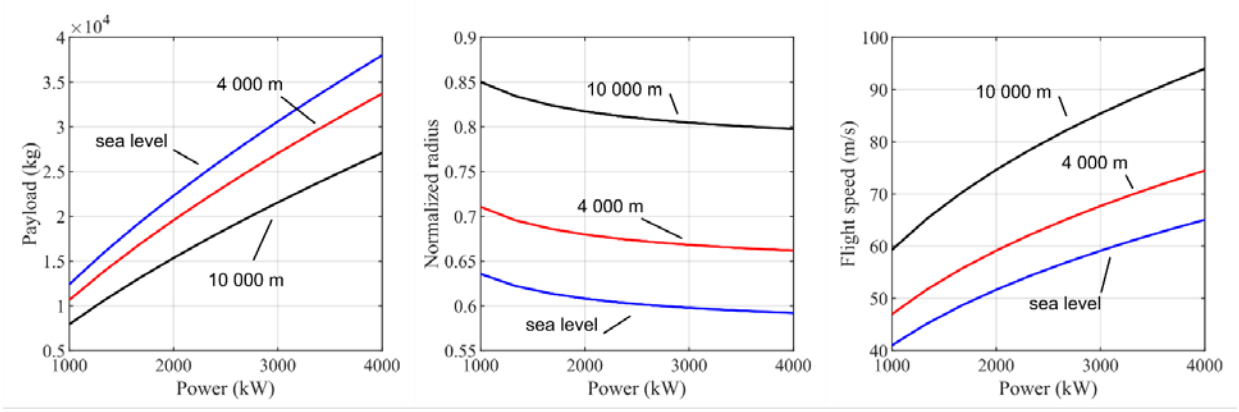

Figure 5.1-5: Effect of altitude on the lifting capability and optimal flight path parameters

A reduction in air density for a given payload increases the power requirement as for a conventional rotorcraft. For a 30-metric ton fuselage, hovering at 4 000 m requires 17% more power, slightly under the momentum theory prediction. However, the airplane flight speed must increase from 58 m/s to 72 m/s and the normalized flight path radius grows from 0.6 to 0.67 (a 11 m increase in actual radius). This behavior provides a near-constant lift coefficient as a function of the operating condition in order to maximize the wing efficiency.

5.2 Sensitivity to Design Assumptions

The work in this paper assumes a fixed tether and airplane design scaled from a large-scale airborne wind turbine. For an increase in the wing mass by 1 metric ton (total mass of 2500 kg) and the tether outside diameter increase of 33% to reach 1 in in diameter, the system lifting capacity is reduced by 8% for a 3 MW power supply. This low sensitivity to the wing mass results from the low “rotor-to-fuselage” mass ratio (16% only) and the capability of the airplane to reconfigure their flight path to minimize the consequence of the increase in mass and tether drag. Alternatively, an increase in the airplane wingspan to 26 m while maintaining a constant chord reduces the power requirement by 17% but increases the ground footprint of the system.

5.3 Series Hybrid-Electric Propulsion Design

Electric propulsion is an enabler for the EPR^2 VTOL concept to achieve vertical takeoff of the tethered airplanes and to provide the required acceleration and deceleration to follow the optimal flight path in the presence of wind. However, current battery technologies cannot provide meaningful range and endurance except for specific very short missions. A series-hybrid powertrain combined with a small battery pack would provide both the performance of fuel-based propulsion systems and flexibility of electric propulsion.

It would be too early to suggest any specific range or endurance for the EPR2 VTOL concept at this stage since a detailed powertrain model and a fuselage mass model have yet to be evaluated. However, assuming a 38% efficient hybrid-electric powertrain (Picard et al., 2019), Figure 5.3-11 details the variation of fuselage mass and fuel burn as a function of time.

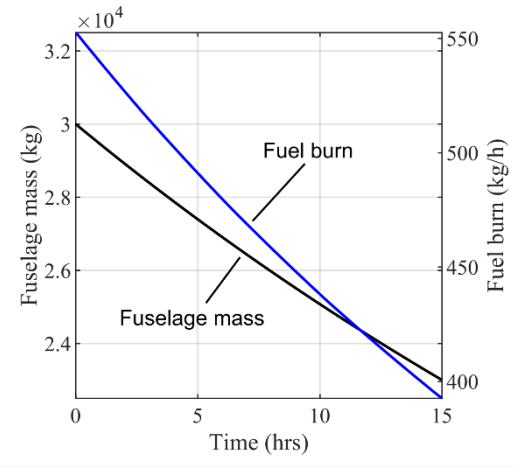

Figure 5.3-11: Fuel burn and fuselage mass decay as a function of time

For an initial fuselage mass of 30 000 kg, a 6000 kg fuel tank could provide in excess of 12 hours endurance in hover, well above any conventional helicopter. Such endurance has also been demonstrated in the AHS Sikorsky graduate student competition (Bass et al., 2019) where a high-efficiency design reaching 30 hours of endurance was presented based on the EPR^2 concept. These new capabilities could support current and future NATO efforts.

6.0 CONCLUSION

This paper presented the performance estimation a heavy-lifting VTOL aircraft based on collaborative load lifting electric-powered using fixed-wing aircraft. This study aimed at the flight path optimization of the tethered airplanes to explore the power requirement in hover and in forward flight, where there is a potential to increase efficiency through complex non-circular flight path.

Based on three tethered fixed-wing aircraft with 20-m span adapted from the airborne energy sector, it is shown that a 30-ton fuselage could be lifted using 3.01 MW electrical power, and a mild increase in the wingspan to 26 m could reduce the power requirement to 2.5 MW. The system can also translate (or hover) up to 80 kts (40 m/s) provided the airplane flight path are optimized using 4 MW.

The system's robustness to design assumption. For an increase of 66% of the airplane mass combined with an increase of 33% in the tether diameter only reduces the lifting capability by 8% thanks to the reconfigurable rotor that adapts to minimize the power requirement.

Electric propulsion and series-hybrid electric powertrain are enablers for the EPR^2 concept due to the strong variation in the power requirement as a function of time in the presence of wind. Using advanced turbogenerators, a 6 000 kg fuel load could enable the EPR^2 to hover in excess of 12 hours.

Although early in the technology development roadmap, the numerical results presented in this paper highlights the potential contribution the EPR^2 can have in military applications. Future work includes experimental flight tests of subscale models including control optimization. Control challenges are expected, but given the radical potential benefits, significant research efforts are worth investing.

7.0 REFERENCES

Ardema, M. D. (1981). *Vehicle Concepts and Technology Requirements for Buoyant Heavy-Lift Systems*. Moffett Field, CA: NASA.

Bass, J. et al. (2019). Preliminary Design of a Highly Efficient VTOL System Based on Tethered Fixed-Wing Aircraft. In: *Vertical Flight Society 75th Annual Forum Proceedings*. May 2019. Philadelphia, PA.

Brown, E. (1981). *The helicopter in civil operations*. London: Granada.

Carichner, G. E. and Nicolai, L. M. (2013). *Fundamentals of Aircraft and Airship Design, Volume 2. Airship Design and Case Studies*, AIAA Education Series. American Institute of Aeronautics and Astronautics, Inc.

Chapdelaine, B., Ledoux, G. and Rancourt, D. (2019). Experimental Validation of Vertical LIfting Capabilities of Circling Tethered Fixed Wing UAVs. In: *Vertical Flight Society 75th Annual Forum Proceedings*. May 2019. Philadelphia, PA.

Demers Bouchard, E., Rancourt, D. and Mavris, D. N. (2015). Design Space Exploration of Reconfigurable Rotor. In: *AHS 71st Annual Forum and Technology Display*. 4 May 2015. Virginia Beach, VA.

Heatley, M. (1985). *The illustrated history of helicopters*. London: Brompton Books Corp.

Hoerner, S. F. (1992). *Fluid-dynamic drag: practical information on aerodynamic drag and hydrodynamic resistance*. Bakersfield: Hoerner Fluid Dynamics.

Johnson, W. (2013). *Rotorcraft aeromechanics*, Cambridge aerospace series 36. Cambridge: Cambridge University Press.

Makani Power. (2011). *Response to the Federal Aviation Authority*.

Picard, B. et al. (2019). Enabling Sub-Megawatt Hybrid-Electric Propulsion through High Efficiency Recuperated Inside-out Ceramic Turbogenerator. In: *Proceedings of the NATO AVT-323 Research Symposium on Hybrid/Electric Aero-Propulsion Systems for Military Applications*. 7 October 2019. Trondheim, Norway.

Rajendran, P., Masral, M. H. and Kutty, H. A. (2017). Perpetual Solar-Powered Flight across Regions around the World for a Year-Long Operation. *Aerospace*, 4 (2), p.20.

Rancourt, D. (2016). *Method for the flight path optimization of the electric-powered reconfigurable rotor (EPR2) VTOL concept*. PhD Thesis, Georgia Institute of Technology.

Rancourt, D., Demers Bouchard, E. and Mavris, D. N. (2016). Optimal Flight Path of the Tethered Airplanes in the EPR2 VTOL Concept During Moderate Flight Velocity. In: *AHS Technical Meeting on Aeromechanics Design for Vertical Lift*. 20 January 2016. San Francisco, CA.

Toliyat, H. A. and Kliman, G. B. (2004). *Handbook of Electric Motors*. CRC Press.

Williams, P. (2010). Optimization of Circularly Towed Cable System in Crosswind. *Journal of guidance, control, and dynamics*, 33 (4), pp.1251–1263.

Williams, P. and Ockels, W. (2009). Dynamics of towed payload system using multiple fixed-wing aircraft. *Journal of guidance, control, and dynamics*, 32 (6), pp.1766–1780.

Williams, P. and Trivailo, P. (2007a). Dynamics of Circularly Towed Aerial Cable Systems, Part 2: Transitional Flight and Deployment Control. *Journal of guidance, control, and dynamics*, 30 (3), pp.766–779.

Williams, P. and Trivailo, P. (2007b). Dynamics of circularly towed aerial cable systems, part I: optimal configurations and their stability. *Journal of guidance, control, and dynamics*, 30 (3), pp.753–765.

Wilson, JR., F. and Bennet, A. (1983). New concept for low cost VTOL cargo delivery capability. In: *Guidance and Control Conference*. 15 August 1983. Gatlinburg, TN: American Institute of Aeronautics and Astronautics.

Wilson Jr., F. M. (1983). *Aerial transport of payloads with vertical pick up and delivery*. Kennesaw, GA.